Dual-band MIMO antenna for wideband THz communication in future 6G applications

Jamal Hossain Nirob[1], Kamal Hossain Nahin[1], Md. Ashraful Haque[1], Md. Sharif Ahammed[1], Narinderjit Singh Sawaran Singh[2], Redwan A. Ananta[1], Md. Kawsar Ahmed[1], Liton Chandra Paul[3]
[1]Department of Electrical and Electronic Engineering, Daffodil International University, Dhaka, Bangladesh
[2]Faculty of Data Science and Information Technology, INTI International University, Nilai, Malaysia
[3]Department of Electrical, Electronic and Communication Engineering, Pabna University of Science and Technology, Pabna, Bangladesh

Article Info

Article history:

Received Aug 7, 2024
Revised Dec 25, 2024
Accepted Jan 23, 2025

Keywords:

6G communication
Industrial and innovation
Multiple-input multiple-output
resistance, inductance, and capacitance
THz antenna
Wide bandwidth

ABSTRACT

This paper presents an industrial and innovation dual-band multiple-input multiple-output (MIMO) antenna designed for terahertz (THz) frequencies to enhance future sixth-generation (6G) communication systems. The antenna utilizes a polyimide substrate with a thickness of 12 µm, a dielectric constant of 3.5 and a tangent loss of 0.0027. Both the patch and the ground plane are constructed from copper, ensuring robust performance. The antenna achieves resonance at 5.45 THz with a gain of 14 dB and a bandwidth of 0.7 THz and at 6.34 THz with a gain of 14.44 dB and a bandwidth of 1.77 THz. Additionally, it demonstrates a minor peak at 7.4 THz and a maximum efficiency of 95.87%. The transmission coefficient shows an isolation of -31.01 dB, indicating excellent separation between antenna elements. Key MIMO performance metrics, containing the envelope correlation coefficient (ECC), diversity gain (DG), mean effective gain (MEG), total active reflection coefficient (TARC), and channel capacity loss (CCL), were analyzed, displaying optimum performance. An analogous circuit was designed and simulated in advanced design system (ADS) to validate these discoveries, creating comparable reflection coefficients to those attained from computer simulation technology (CST) simulations. These findings approve the antenna's possible for THz-band 6G wireless communication applications.

Corresponding Author:

Narinderjit Singh Sawaran Singh
Faculty of Data Science and Information Technology, INTI International University
Persiaran Perdana BBN, Putra Nilai, Nilai 71800, Negeri Sembilan, Malaysia
Email: narinderjits.sawaran@newinti.edu.my

1. INTRODUCTION

The beginning of sixth-generation (6G) wireless communication scripts a transformative leap in connectivity, gifted to revolutionise how we narrate with technology and the world around us [1]. 6G technology can spread the aptitudes of current wireless systems by contributing faster speeds and more reliable connections, allowing new use cases that contain real-time, high-bandwidth communication [2]. For example, in immersive virtual reality, 6G can deliver the ultra-fast data transmission desirable for all-in-one, high-definition experiences [3]. Independent systems, self-driving cars, and drones will benefit from 6G's low latency, vital for real-time decision-making and safe process [4]. Additionally, the Internet of Everything will see an ignition of connected devices needing efficient and reliable communication links, which 6G can provide. Essential to achieving the determined goals of 6G is utilising the terahertz (THz) frequency range, which ranges from 0.1 THz to 10 THz [5]. This mostly unused spectrum offers a vast bandwidth potential, making it restful for meeting the high-speed, high-capacity necessities of 6G networks [6]. THz frequencies are attractive for wireless communication since they provide multi-gigabit-per-second (Gbps) data rates and ultra-low latency [7]. These characteristics are essential for supportive data-intensive and delay-sensitive applications intended for 6G, such as remote surgery, real-time holographic communications, and advanced manufacturing processes [8].

The design of efficient and high-performance antennas is one of the critical challenges in harnessing THz frequencies for 6G wireless communication. Mixing multiple-input multiple-output (MIMO) technology with THz frequencies offers several advantages, including improved channel capacity, better signal quality, and enhanced coverage [9]. MIMO systems influence multiple antennas at both the transmitter and receiver to create multiple communication paths, effectually multiplying the capacity of the wireless channel [10]. The development of THz MIMO antennas is important for realizing the full potential of 6G wireless communication. These antennas will play an essential role in delivering the ultra-fast, high-capacity, and low-latency connectivity required to support the varied and challenging applications of the future [11]. The study and advancement of THz antenna technology will pave the way for a new period of wireless communication, altering how we connect and cooperate in the digital age [12].

Table 1 presents a proportional analysis of various MIMO antenna designs, converging on their essential parameters and performance metrics. The analysis covers bandwidth, isolation, gain, efficiency, envelope correlation coefficient (ECC), diversity gain (DG), and the inclusion of resistance, inductance, and capacitance (RLC) circuits. The proposed antenna demonstrates remarkable performance across these parameters, showcasing significant advancements in antenna technology.

Table 1. Performance comparison with related works

Ref	Resonance (THz)	BW (THz)	Isolation (dB)	Gain (dB)	Efficiency (%)	ECC, DG (dB)	Substrate material	Port	RLC
[13]	0.654	0.05	≥ 25	11.67	76.45%	0.003, 9.99	Polyimide	-	No
[14]	-	0.114	-17	4.4	94	0.006, 9.97	Rogers RO4835-T	4	No
[15]	8.84	0.0404	−22.26	8.2	-	0.0005, 9.995	RT/Duroid/6010	4	No
[16]	1.9	0.3	-35	10	-	0.000023/9.99	Polyimide	2	Yes
[17]	2.2	0.78	-20	4.4	96	0.006, 9.9998	Polyimide	2	Yes
[18]	-	0.11	-25	4.45	-	0.0372,9.99	Silicon dioxide	2	No
Proposed	5.45, 6.34	0.7, 1.77	-30.6, -31.01	14, 14.44	91.03, 95.87	0.0003, 9.998	Polyimide	2	Yes

Bandwidth values show considerable variation, with measurements including 0.05 THz, 0.114 THz, 0.0404 THz, 0.3 THz, 0.78 THz, and 0.11 THz [13]-[18]. The proposed design attains pointedly broader bandwidths of 0.7 THz and 1.77 THz at its two resonance frequencies, which is important because of its capacity to conceal a wide frequency range. Referenced gains from former works, such as 11.67 dB, 4.4 dB, 8.2 dB, 10 dB, 4.4 dB, and 4.45 dB, are providing [13]-[18]. In distinction, the proposed design achieves considerably higher gains of 14 dB and 14.44 dB at its two resonance frequencies. Isolation levels in the proposed layout surpass -30 dB at both resonance frequencies, which is an improvement compared to the measured levels of -25 dB, -17 dB, -22.26 dB, -35 dB, -20 dB, and -25 dB in the cited sources [13]-[18]. The efficiency of the proposed design is 91.03% at the first band and 95.87% at the second band, surpassing efficiencies of 76.45%, 94%, and 96% cited in studies [13], [14], [17].

The proposed MIMO antenna demonstrated outstanding performance compared to other alternatives, with an ECC below 0.0003 and a DG exceeding 9.998. Notably, while references [16], [17] incorporated RLC circuits, the proposed antenna integrates RLC components to analyze its electromagnetic behaviour, setting it apart and highlighting its innovative approach. These features collectively showcase the proposed antenna's potential to lead the field of antenna technology and drive future advancements, making it the best among the compared designs.

2. ITERATIVE DESIGN AND ANALYSIS OF PROPOSED SINGLE-ELEMENT ANTENNA

We meticulously designed a single-element antenna to develop a state-of-the-art one for THz applications, refining its structure through three iterative stages to achieve optimal performance. This section details the design methodology. We selected polyimide as the substrate, praised for its superior dielectric properties, including a dielectric constant 3.5 and a low-loss tangent of 0.0027 [19]. Copper was applied individually to the patch and ground elements, confirming ideal conductivity and performance. A full-ground plane was steadily employed throughout the design. Figure 1(a) shows the reflection coefficient at each step, Figure 1(b) depicts the respective gain, and Figure 1(c) presents the final antenna design. At first, we executed a trapezium-shaped patch with a feedline. Two resonance frequencies caused this configuration with a bandwidth of 1.2 THz, but both return loss and gain were suboptimal. As for the second stage, we offered two insets on either side of the feedline and added a pole at the top-left corner of the trapezium. This design generated a single resonance frequency and improved gain and return loss, though the bandwidth remained inadequate.

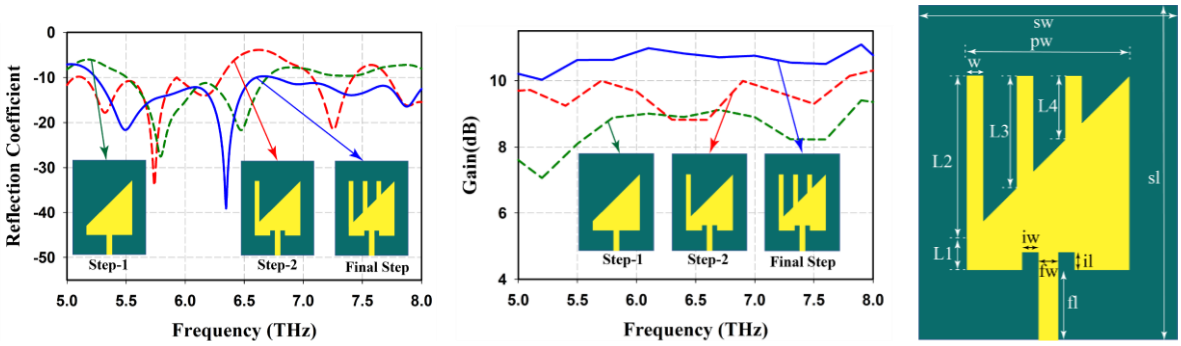

(a) (b) (c)

Figure 1. Analysis of the single-element antenna: (a) S11 comparison, (b) comparison of gain across three steps, and (c) front view of the single-element antenna

At the final stage, we further refined the design by including extra geometric changes, including two new poles—one at the centre and another at the right side of the trapezium's top edge. This final arrangement achieved a resonance frequency of 6.33 THz, with a return loss of -37.36 dB and a lingering bandwidth of 1.4 THz. The gain was improved to 11 dB, marking a noteworthy advancement in performance. These improvements condense the antenna highly suitable for next-generation communication technologies and high-resolution THz imaging.

3. DESIGN AND ANALYSIS OF MIMO ANTENNA

MIMO technology drives wireless communication systems, particularly for 6G. This leads to enhanced spectral efficiency and sturdiness, making it possible to support a higher density of users and more complex data streams, which is critical for the demanding requirements of 6G applications [20]. This section details the progression from a single-element antenna to a 2-port MIMO antenna. Figure 2(a) depicts the proposed MIMO configuration, where two polarized antenna elements are oriented perpendicularly. These elements are spaced 53 μm apart edge-to-edge, within overall dimensions of 185×185 μm^2. This precise arrangement optimizes spatial diversity and reduces mutual coupling, enhancing signal quality and reliability.

Figure 2(b) compares the return loss between the single-element and MIMO antennas, clearly showing that the MIMO antenna achieves dual-band operation. In contrast, the single-element antenna supports only a single band. The first resonance frequency for the MIMO antenna occurs at 5.45 THz, with a notable bandwidth of 0.7 THz, and the second resonance band appears at 6.34 THz, featuring a bandwidth of 1.77 THz. This indicates a significant improvement in bandwidth for the MIMO antenna, which also shows enhanced return loss compared to the single-element antenna. The resonance frequencies of the two bands in the MIMO antenna closely match those of the single-element design. However, the MIMO antenna introduces a minor peak at 7.4 THz, indicating strong performance at higher frequencies.

Figure 2(c) also highlights the comparison between single-element gain and MIMO antennas. The MIMO antenna achieves a gain of 14 dB in the first band and 14.44 dB in the second band, compared to a maximum gain of 11 dB in the single-element antenna. This performance improvement demonstrates that the MIMO configuration suits next-generation communication technologies and high-resolution THz imaging. These values represent the ideal setting of the antenna, sw=80 μm, sl=103 μm, L1=10 μm, L2=20 μm, L3=35 μm, L4=20 μm, w=5 μm, pw=50 μm, iw=5 μm, il=5 μm, fl=21.5 μm, fw=6 μm, D=120 μm, SW=SL=185 μm.

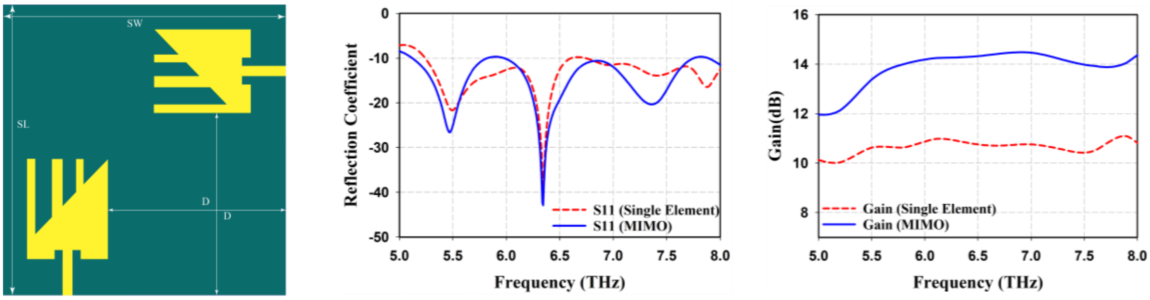

(a) (b) (c)

Figure 2. MIMO antenna overview: (a) MIMO antenna design, (b) S11 parameter, and (c) gain

4. RESULTS ANALYSIS OF THE RECOMMENDED MIMO ANTENNA

4.1. Reflection coefficient and transmission coefficient analysis

The reflection coefficient, often represented as S11 or return loss, measures how much power is reflected from the antenna [21]. It is a crucial parameter in antenna design. For the designed patch antenna, the reflection coefficient indicates strong performance in dual bands, as depicted in Figure 3(a). The first resonance frequency is at 5.45 THz with a return loss of -27 dB, operating between 5.11 THz and 5.81 THz, providing a substantial bandwidth of 0.7 THz. The second resonance band is observed at 6.34 THz with an impressive return loss of -43 dB. This band operates from 5.98 THz to 7.75 THz, offering a large bandwidth of 1.77 THz. Additionally, a minor peak at 7.4 THz with a return loss of -20.207 dB is noted within this band, indicating good performance even at higher frequencies. The significant return loss values in both bands suggest that the antenna is highly efficient in its intended frequency ranges and matched to the transmission line.

Regarding the transmission coefficient or isolation, which is represented as S21 or S12, the proposed MIMO antenna achieves an isolation of -31.01 dB, as shown in Figure 3(b). The transmission coefficient indicates the level of power that is coupled from one antenna element to another. A lower transmission coefficient value (more negative in dB) corresponds to higher isolation. This high isolation value indicates excellent separation between antenna elements, minimizing interference and enhancing overall system performance [22].

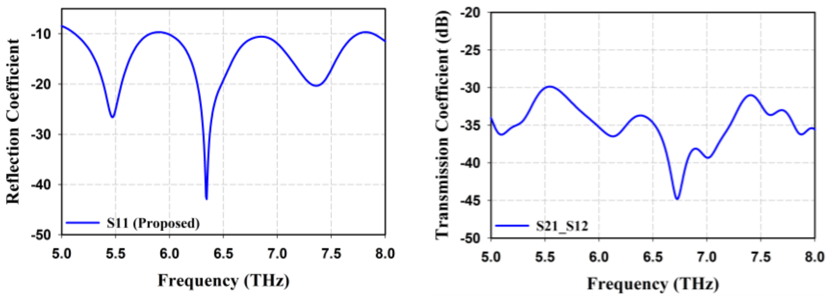

(a) (b)

Figure 3. Performance analysis of the proposed MIMO antenna: (a) reflection and (b) transmission coefficient

4.2. Gain and efficiency

Gain and efficiency are important parameters for estimating the performance of an antenna [23]. Gain states to the ability of the antenna to straight or pay attention to radio frequency energy in a certain direction, though efficiency measures how efficiently the antenna adapts input power into radiated power [24]. Figure 4 shows a plot of the simulated gain and Efficiency of the proposed antenna.

The designed antenna demonstrates excellent recital in terms of gain and efficiency. It attains a maximum gain of 14.5 dB transversely to the operating range, with precise gains of 14 dB at 5.45 THz and 14.44 dB at 6.34 THz, as shown in Figure 4(a). These high gain values specify that the antenna effectively directs energy, which is helpful for long-distance communication and high-resolution imaging applications in the THz range [25].

Additionally, the antenna displays a maximum radiation efficiency of 95.87% at 6.34 THz and 89.93% at 5.45 THz. Additionally, the total efficiency of the antenna is 95.43% at 6.34 THz and 89.85% at 5.45 THz, as shown in Figure 4(b). These efficiency values are quite high, suggesting that the antenna has minimal power losses and can effectively radiate the input power.

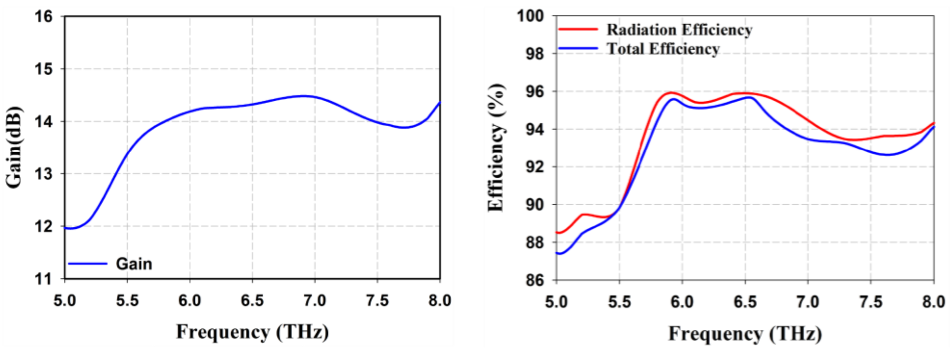

(a) (b)

Figure 4. Performance evaluation of the proposed MIMO antenna: (a) gain and (b) efficiency

4.3. Diversity performance analysis

ECC measures the correlation amid signals received or emitted by various antenna essentials. The value of ECC can be figured out by using the (1) [26]:

$$\frac{\left|\int_{4\pi}[E_1(\theta,\varphi)*E_2(\theta,\varphi)]d\Omega\right|^2}{\int_{4\pi}|E_1(\theta,\varphi|^2 d\Omega \int_{4\pi}|E_2(\theta,\varphi|^2 d\Omega} \tag{1}$$

where the two antennas' complex electric field patterns are denoted by E1 (θ, ϕ) and E2 (θ, ϕ). The solid angle (Ω) over a sphere is comprised of the azimuth angle (ϕ) and the elevation angle (θ). The differential element of the solid angle is denoted by dΩ. The integrals are calculated across the whole sphere, indicated by 4π.

Figure 5(a) illustrates that the designed antenna has an ECC value of 0.0003, which is remarkably low and highly desired. A low ECC value ensures effective diversity performance and reduces the chances of signal fading. DG specifies the enhancement in signal quality due to diversity. The value of DG can be determined by using the equation provided here [27].

$$DG = 10\sqrt{1-ECC^2} \tag{2}$$

Figure 5(b) depicts that the achieved DG value is 9.9998, close to the ideal value of 10. This high DG value signifies that the antenna system provides excellent diversity gain, enhancing the reliability and robustness of the communication link [28].

When an antenna is subjected to uniformly arriving signals from all directions, taking into consideration fading and polarization effects in a wireless communication environment, the average gain is known as mean effective gain (MEG). The MEGs of the two antenna elements vary from 7.8 dB to 5.8 dB over the whole frequency spectrum, as shown in Figure 6(a). The variation of MEGs, indicated by the k=power ratio, ranges from 0 dB to 0.3 dB within the band. It can be mathematically represented as (3) and (4).

$$k = min\left(\frac{MEG_1}{MEG_2}, \frac{MEG_2}{MEG_1}\right) \tag{3}$$

$$MEG_i = 0.5\left[1 - \sum_{J=1}^{N} S_{ij}\right] \tag{4}$$

The channel capacity loss (CCL) is measured in bits/s/Hz, which measures the information loss due to mutual coupling between other antennas. If the CCL value is lower the information loss will be less. As for our proposed MIMO antenna the CCL we get is near to Zero which indicate that the information loss is also less that shown in Figure 6(b).

The suggested MIMO antenna's reflection effectiveness is represented by the total active reflection coefficient (TARC), which is displayed in dB in Figure 6(c). For the suggested antenna, the TARC simulated outputs are shown as < -10 dB. As The TARC values is lower at resonance frequency, which indicate that the proposed antenna has better efficiency. The 3 can be utilized to ascertain this.

$$TARC = \frac{\sqrt{(|S_{xx}|+|S_{xy}|)^2+(|S_{yx}|+|S_{yy}|)^2}}{\sqrt{4}} \quad (5)$$

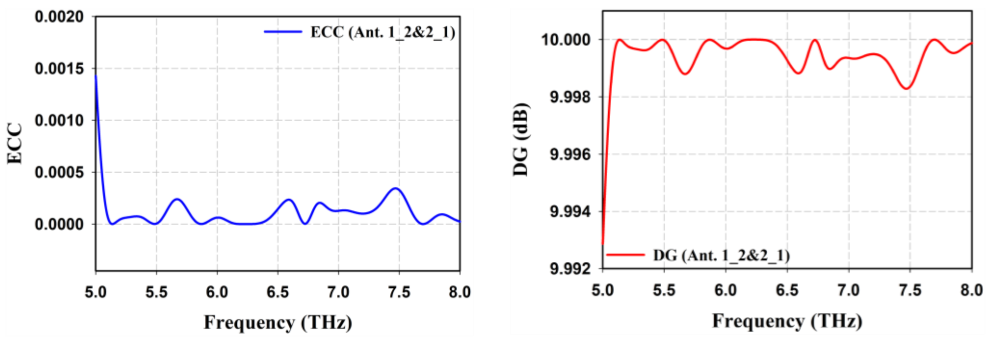

(a) (b)

Figure 5. Diversity performance of the MIMO antenna: (a) ECC and (b) DG

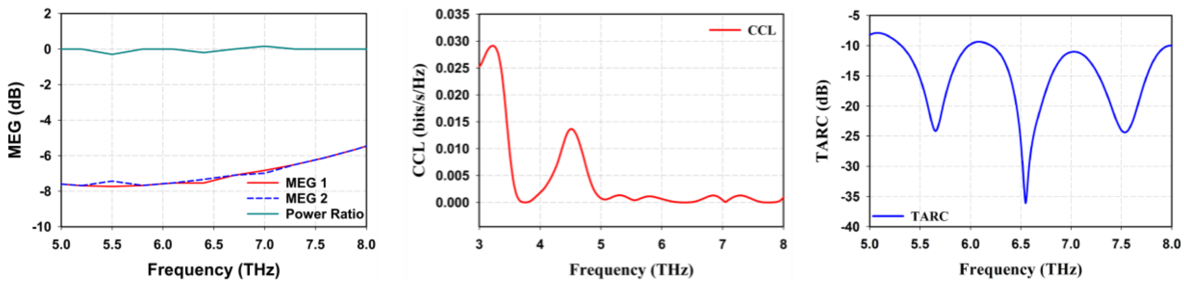

(a) (b) (C)

Figure 6. Diversity performance: (a) MEG, (b) CCL, and (c) TARC of the MIMO antenna

4.4. Radiation pattern

The radiation pattern of the proposed antenna at port-1, operating at the resonance frequency of 6.34 THz, shows distinct characteristics in both the E-field and H-field components, as shown in Figure 7. At port 1, the E-field's main lobe magnitude at ϕ=0° is 16.2 dBV/m with a 3 dB beamwidth of 22.5°, while the H-field has a magnitude of -42.3 dBA/m with a beamwidth of 16.4°. At ϕ=90°, the E-field's magnitude is 12.1 dBV/m with a 19.8° beamwidth, and the H-field is -25.5 dBA/m with a 28.9° beamwidth. For θ=90°, the E-field reaches 26 dBV/m with a beamwidth of 19.4°, and the H-field is -37.5 dBA/m with a 10.3° beamwidth. The radiation pattern analysis reveals notable differences in port-2. At port 2, for the E-field, the main lobe magnitude at ϕ=0° is 11.7 dBV/m, with a 3 dB beamwidth of 79.4°, indicating a relatively broad beam in this plane. At ϕ=90°, the main lobe magnitude increases to 16.4 dBV/m, with a narrower 3 dB beamwidth of 21°, reflecting a more focused beam in the perpendicular plane [29]. Regarding θ=90°, the E-field's main lobe magnitude reaches 25.8 dBV/m, with a half-power beamwidth of 19.3°, demonstrating significant directivity in this direction. Conversely, the H-field's main lobe magnitude at ϕ=0° is -25.9 dBA/m with a 3 dB beamwidth of 28.8°, while at ϕ=90°, the magnitude is -42.5 dBA/m with a 10.8° beamwidth, illustrating a more confined radiation pattern. For θ=90°, the H-field's main lobe magnitude is -40.8 dBA/m with a 21.2° beamwidth, display a comparatively wider beam in this plane compared to the E-field.

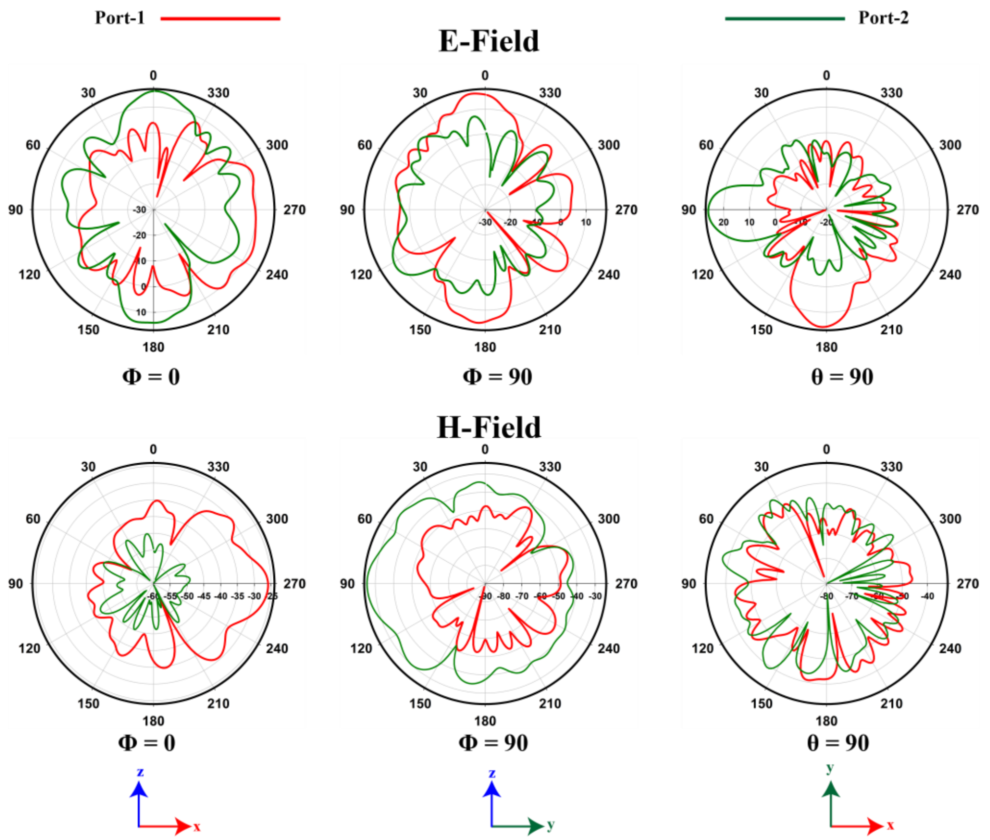

Figure 7. Simulated radiation pattern

5. EQUIVALENT CIRCUIT MODELLING AND SIMULATION

In our pursuit of developing antenna technology, we analyzed the antenna's electromagnetic behaviour using an RLC circuit model. Utilizing CST Studio, we mined detailed R-L-C parameters from our antenna simulations. Agilent ADS circuit simulation was used to optimize the antenna further, allowing a thorough analysis of its behavior [30].

The RLC equivalent circuit design intricate a methodical trial-and-error method within the ADS software, where we iteratively accustomed the RLC parameters to attain optimal results. We carefully adjusted the RLC parameters to achieve ideal performance, certifying the circuit accurately signified the antenna's operational frequency. This was accomplished through a parallel circuit arrangement that included resistance (R1), inductance (L1), and capacitance (C1), sideways with an additional parallel circuit comprising R2, C2, and L2. Furthermore, each pole at the top of the patch was represented by distinct parallel circuits where L3 and C3 represent the left pole, L4 and C4 for the middle pole, and L5 and C6 for the right pole. C6 and C8 denoted capacitances between the left and middle poles, while C7 and C9 represented the capacitances between the middle and right poles. The feedline was incorporated with resistance (R3), capacitance (C10), and inductance (L6), accurately capturing its electrical characteristics. By integrating these individual circuit elements, we constructed a model that mirrored the behaviour of our single-element antenna. Finally, the model extended to a MIMO antenna, as shown in Figure 8, using the single-element circuit as a foundation. Extending this model to a MIMO configuration, we accounted for mutual impedance between antenna elements through a parallel circuit of L7 and C12, optimizing performance evaluation. Simulating the R-L-C circuit model in Agilent ADS, we validated its equivalence to our antenna design. To ensure precision, we compared the outcomes of the CST simulation with the parallel circuit simulation results, focusing on the S11 parameter. Figure 9 illustrates this comparison, thoroughly assessing the accuracy of our R-L-C circuit model in representing the antenna's behavior. It is evident from Figure 9 that the S11 responses of both the CST-designed antenna and the equivalent circuit model using ADS align closely, reinforcing the validity of the equivalent circuit in accurately modelling the antenna's performance.

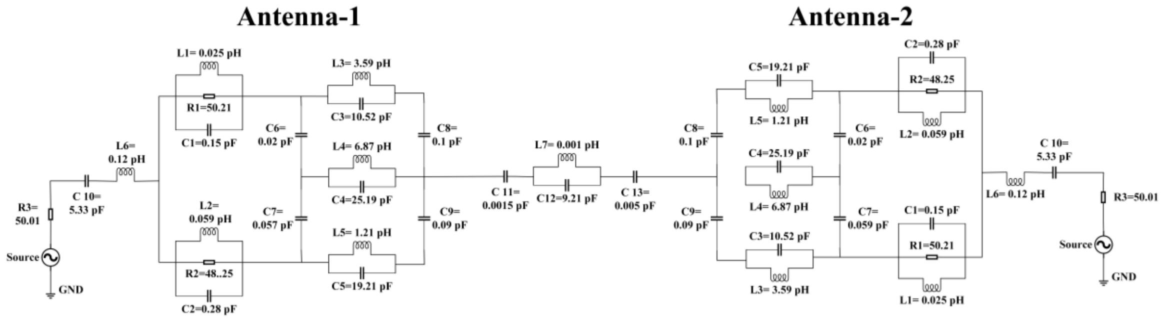

Figure 8. RLC equivalent circuit diagram for the suggested MIMO antenna

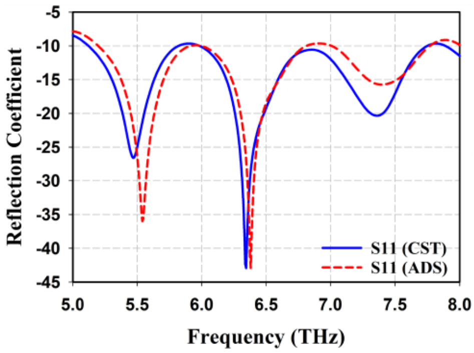

Figure 9. Comparative plot of S11 parameter from CST and ADS simulations

6. CONCLUSION

This research evaluated the effectiveness of the suggested MIMO patch antenna intended for THz frequency applications using various techniques. Using advanced modelling techniques, we thoroughly analysed the antenna's characteristics and developed an RLC-equivalent circuit model. The simulations, performed using ADS and CST software, revealed a remarkable consistency in the antenna's bandwidth, confirming the reliability and precision of our design. The antenna exhibited outstanding performance in critical parameters such as reflection coefficient, gain, efficiency, ECC, and DG, supporting dual-band operation with efficient signal transmission and reception. The high gain and efficiency and minimal signal correlation indicated by the low ECC value affirm the antenna's capability to support high-quality communication and imaging applications in the THz spectrum. The consistent simulation results validate the antenna's potential for integration into advanced communication systems. This study confirms the proposed antenna's viability for THz applications and provides a foundation for future advancements in high-frequency antenna technologies. Future research could focus on integrating massive MIMO technology to enhance system capacity and coverage. Additionally, exploring metamaterials could lead to further performance improvements and novel functionalities. Another promising direction involves applying machine learning techniques to enhance the MIMO antenna's performance further. By collecting extensive data samples, we aim to use deep learning models such as artificial neural network (ANN) and convolutional neural network (CNN) to predict and optimize various antenna parameters, improving future outcomes. The findings of this study contribute significantly to the field and pave the way for future innovations in THz sensing and communication technology.

ACKNOWLEDGEMENT

The author acknowledges the collaboration of the Department of Electrical and Electronic Engineering and the Faculty of Graduate Studies at Daffodil International University in Bangladesh.

REFERENCES

[1] M. Abd Elaziz *et al.*, "Evolution toward intelligent communications: Impact of deep learning applications on the future of 6G technology," *WIREs Data Mining and Knowledge Discovery*, vol. 14, no. 1, p. e1521, Jan. 2024, doi: 10.1002/widm.1521.

[2] H. Vettikalladi, W. T. Sethi, A. F. B. Abas, W. Ko, M. A. Alkanhal, and M. Himdi, “Sub-THz antenna for high-speed wireless communication systems,” *International Journal of Antennas and Propagation*, vol. 2019, pp. 1–9, Mar. 2019, doi: 10.1155/2019/9573647.
[3] R. Chataut, M. Nankya, and R. Akl, “6G networks and the AI revolution—exploring technologies, applications, and emerging challenges,” *Sensors*, vol. 24, no. 6, p. 1888, Mar. 2024, doi: 10.3390/s24061888.
[4] H.-J. Song and N. Lee, “Terahertz communications: challenges in the next decade,” *IEEE Transactions on Terahertz Science and Technology*, vol. 12, no. 2, pp. 105–117, Mar. 2022, doi: 10.1109/TTHZ.2021.3128677.
[5] M. A. Jamshed, A. Nauman, M. A. B. Abbasi, and S. W. Kim, “Antenna selection and designing for THz applications: suitability and performance evaluation: a survey,” *IEEE Access*, vol. 8, pp. 113246–113261, 2020, doi: 10.1109/ACCESS.2020.3002989.
[6] M. F. Ali, R. Bhattacharya, and G. Varshney, “Tunable four-port MIMO/self-multiplexing THz graphene patch antenna with high isolation,” *Optical and Quantum Electronics*, vol. 54, no. 12, p. 822, Dec. 2022, doi: 10.1007/s11082-022-04200-x.
[7] O. A. Amodu, C. Jarray, S. A. Busari, and M. Othman, “THz-enabled UAV communications: motivations, results, applications, challenges, and future considerations,” *Ad Hoc Networks*, vol. 140, p. 103073, Mar. 2023, doi: 10.1016/j.adhoc.2022.103073.
[8] P. Das, “Beam-steering of THz MIMO antenna using graphene-based intelligent reflective surface,” *Optical and Quantum Electronics*, vol. 55, no. 8, p. 711, Aug. 2023, doi: 10.1007/s11082-023-04996-2.
[9] N. Kiani, F. Tavakkol Hamedani, and P. Rezaei, “Graphene-based quad-port MIMO reconfigurable antennas for THz Applications,” *Silicon*, Mar. 2024, doi: 10.1007/s12633-024-02939-4.
[10] P. Tiwari, V. Gahlaut, M. Kaushik, P. Rani, A. Shastri, and B. Singh, “Advancing 5G connectivity: a comprehensive review of MIMO antennas for 5G applications,” *International Journal of Antennas and Propagation*, vol. 2023, pp. 1–19, Aug. 2023, doi: 10.1155/2023/5906721.
[11] O. A. Amodu, S. A. Busari, and M. Othman, “Physical layer aspects of terahertz-enabled UAV communications: challenges and opportunities,” *Vehicular Communications*, vol. 38, p. 100540, Dec. 2022, doi: 10.1016/j.vehcom.2022.100540.
[12] M. H. Maktoomi, Z. Wang, H. Wang, S. Saadat, P. Heydari, and H. Aghasi, “A sub-terahertz wideband stacked-patch antenna on a flexible printed circuit for 6G applications,” *IEEE Transactions on Antennas and Propagation*, vol. 70, no. 11, pp. 10047–10061, Nov. 2022, doi: 10.1109/TAP.2022.3185497.
[13] R. Pant and L. Malviya, “Terahertz MIMO antenna array for future generation of wireless applications,” *Frequenz*, vol. 78, no. 5–6, pp. 271–280, Jun. 2024, doi: 10.1515/freq-2023-0203.
[14] T. Okan, “High efficiency unslotted ultra-wideband microstrip antenna for sub-terahertz short range wireless communication systems,” *Optik*, vol. 242, p. 166859, Sep. 2021, doi: 10.1016/j.ijleo.2021.166859.
[15] Q. Rubani, S. H. Gupta, and A. Rajawat, “A compact MIMO antenna for WBAN operating at Terahertz frequency,” *Optik*, vol. 207, p. 164447, Apr. 2020, doi: 10.1016/j.ijleo.2020.164447.
[16] S. A. Khaleel, E. K. I. Hamad, N. O. Parchin, and M. B. Saleh, “Programmable beam-steering capabilities based on graphene plasmonic THz MIMO antenna via reconfigurable intelligent surfaces (RIS) for IoT applications,” *Electronics*, vol. 12, no. 1, p. 164, Dec. 2022, doi: 10.3390/electronics12010164.
[17] A. Kumar, D. Saxena, P. Jha, and N. Sharma, “Compact two-port antenna with high isolation based on the defected ground for THz communication,” *Results in Optics*, vol. 13, p. 100522, Dec. 2023, doi: 10.1016/j.rio.2023.100522.
[18] G. Varshney, S. Gotra, V. S. Pandey, and R. S. Yaduvanshi, “Proximity-coupled two-port multi-input-multi-output graphene antenna with pattern diversity for THz applications,” *Nano Communication Networks*, vol. 21, p. 100246, Sep. 2019, doi: 10.1016/j.nancom.2019.05.003.
[19] D. Ziani, M. Belkheir, M. Rouissat, and A. Mokaddem, “Design optimization for improving the performance of rectangular antennas using polyimide (PI) and liquid crystal (LC) polymers substrates,” *Polymer Bulletin*, vol. 81, no. 9, pp. 8447–8469, Jun. 2024, doi: 10.1007/s00289-023-05114-8.
[20] G. Saxena *et al.*, “Metasurface inspired wideband high isolation THz MIMO antenna for nano communication including 6G applications and liquid sensors,” *Nano Communication Networks*, vol. 34, p. 100421, Dec. 2022, doi: 10.1016/j.nancom.2022.100421.
[21] Md. K. Ahmed *et al.*, “ANN-based performance estimation of a slotted inverted F-shaped tri-band antenna for satellite/mm-wave 5G application,” *TELKOMNIKA Telecommunication, Computing, Electronics and Control*, vol. 22, no. 4, pp. 773-783, Aug. 2024, doi: 10.12928/telkomnika.v22i4.26028.
[22] U. Raj, M. K. Sharma, V. Singh, S. Javed, and A. Sharma, “Easily extendable four port MIMO antenna with improved isolation and wide bandwidth for THz applications,” *Optik*, vol. 247, p. 167910, Dec. 2021, doi: 10.1016/j.ijleo.2021.167910.
[23] Md. A. Haque *et al.*, “Broadband high gain performance MIMO antenna array for 5 G mm-wave applications-based gain prediction using machine learning approach,” *Alexandria Engineering Journal*, vol. 104, pp. 665–679, Oct. 2024, doi: 10.1016/j.aej.2024.08.025.
[24] Md. A. Haque, L. C. Paul, R. Azim, Md. M. Mowla, A. Saleh, and Md. N. Hossain, “A Modified e-shaped microstrip patch antenna for C band satellite applications,” in *2019 IEEE International Conference on Signal Processing, Information, Communication & Systems (SPICSCON)*, Dhaka, Bangladesh: IEEE, Nov. 2019, pp. 27–31, doi: 10.1109/SPICSCON48833.2019.9065126.
[25] M. A. Haque, L. C. Paul, S. Kumar, R. Azim, Md. S. Hosain, and M. Azman Zakariya, “A plowing T-shaped patch antenna for WiFi and C band applications,” in *2021 International Conference on Automation, Control and Mechatronics for Industry 4.0 (ACMI)*, Rajshahi, Bangladesh: IEEE, Jul. 2021, pp. 1–4, doi: 10.1109/ACMI53878.2021.9528266.
[26] A. A. Althuwayb *et al.*, “Broadband, high gain 2×2 spiral shaped resonator based and graphene assisted terahertz MIMO antenna for biomedical and WBAN communication,” *Wireless Networks*, vol. 30, no. 1, pp. 495–515, Jan. 2024, doi: 10.1007/s11276-023-03494-3.
[27] V. Sorathiya *et al.*, “Graphene-based log-periodic dipole antenna-shaped MIMO antenna structure for the terahertz frequency spectrum,” *Arabian Journal for Science and Engineering*, vol. 49, no. 5, pp. 6391–6404, May 2024, doi: 10.1007/s13369-023-08235-4.
[28] M. Srinubabu and N. V. Rajasekhar, “Enhancing diversity and isolation performance for a four-port MIMO antenna in FR-1 5G frequency bands,” *IETE Journal of Research*, pp. 1–16, Mar. 2024, doi: 10.1080/03772063.2024.2324025.
[29] M. M. Fakharian, “A graphene-based multi-functional terahertz antenna,” *Optik*, vol. 251, p. 168431, Feb. 2022, doi: 10.1016/j.ijleo.2021.168431.
[30] L. C. Paul, M. A. Haque, M. A. Haque, M. M. U. Rashid, M. F. Islam, and M. M. Rahman, “Design a slotted metamaterial microstrip patch antenna by creating three dual isosceles triangular slots on the patch and bandwidth enhancement,” in *2017 3rd International Conference on Electrical Information and Communication Technology (EICT)*, Khulna: IEEE, Dec. 2017, pp. 1–6, doi: 10.1109/EICT.2017.8275143.

BIOGRAPHIES OF AUTHORS

Jamal Hossain Nirob is a student in the Department of Electrical and Electronic Engineering (EEE) at Daffodil International University. His educational journey began at Maniknagar High School, where he successfully completed his Secondary School Certificate (SSC). Following that, he pursued higher studies at Ishwardi Government College, obtaining his Higher Secondary Certificate (HSC). With a strong enthusiasm for expanding communication technology. He has focused his research on wireless communication, specifically on microstrip patch antennas, terahertz antennas, and applications of 5G and 6G. He can be contacted at email: jamal33-1243@diu.edu.bd.

Kamal Hossain Nahin currently pursuing a degree in Electrical and Electronic Engineering at Daffodil International University. His educational journey commenced at Ishwardi Govt College for Higher Secondary Certificate (HSC) and earlier at Maniknagar High School for Secondary School Certificate (SSC). Embarking on a journey as a budding researcher in the communication field. He is passionately immersed in exploring the realms of wireless communication. His focus lies in delving into the intricacies of wireless communication, particularly exploring microstrip patch antennas, terahertz antennas, and their potential applications in the future realms of 5G and 6G technologies. He can be contacted at email: kamal33-1242@diu.edu.bd.

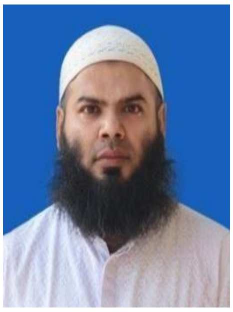

Md. Ashraful Haque is doing Ph.D. at the Department of Electrical and Electronic Engineering, Universiti Teknologi PETRONAS, Malaysia. He got his B.Sc. in Electronics and Electronic Engineering (EEE) from Bangladesh's Rajshahi University of Engineering and Technology (RUET) and his M.Sc. in the same field from Bangladesh's Islamic University of Technology (IUT). He is currently on leave from Daffodil International University (DIU) in Bangladesh. His research interest includes microstrip patch antenna, sub 6 5G application, and supervised regression model machine learning on antenna design. He can be contacted at email: limon.ashraf@gmail.com.

Md. Sharif Ahammed is a student of Daffodil International University and pursuing a B.Sc. in the Department of Electrical and Electronics. He passed from Government Bangabandhu College with a higher secondary. Microstrip patch antenna, terahertz antenna, and 5G application, and biomedical applications are some of his research interests. He can be contacted at email: sharif33-1152@diu.edu.bd.

Narinderjit Singh Sawaran Singh is a Associate Professor in INTI International University, Malaysia. He graduated from the Universiti Teknologi PETRONAS (UTP) in 2016 with Ph.D. in Electrical and Electronic Engineering specialized in probabilistic methods for fault tolerant computing. Currently, he is appointed as the research cluster head for computational mathematics, technology and optimization which focuses on the areas like pattern recognition and symbolic computations, game theory, mathematical artificial intelligence, parallel computing, expert systems and artificial intelligence, quality software, information technology, exploratory data analysis, optimization algorithms, stochastic methods, data modelling, and computational intelligence-swarm intelligence. He can be contacted at email: narinderjits.sawaran@newinti.edu.my.

Redwan A. Ananta has accomplished his undergraduate studies in the field of Electrical and Electronics at Daffodil International University. He completed his higher secondary education at Adamjee Cantonment College. His research focus encompasses wireless communication, specifically microstrip patch antenna, terahertz antenna, and 5G, and 6G applications. He can be contacted at email: redwan33-1145@diu.edu.bd.

Md. Kawsar Ahmed is currently pursuing his studies in the field of Electrical and Electronic Engineering at Daffodil International University. He successfully finished his Higher Secondary education at Agricultural University College, Mymensingh. He is presently employed as an Assistant Administrative Officer at the Office of Students' Affairs at Daffodil International University (DIU) in Bangladesh. The areas of his research focus encompassed microstrip patch antennas, terahertz antennas, and applications related to 4G and 5G technologies. He can be contacted at email: kawsar33-1241@diu.edu.bd.

Liton Chandra Paul (SMIEEE) successfully completed his Master's in Electrical and Electronic Engineering (EEE) in 2012 and his Bachelor's in Electronics and Telecommunication Engineering (ETE) in 2015. As a student, he actively contributed to various nonprofit organizations. He currently serves as an advisor for IEEE PUST SB and IEEE PUST AP-S SB Chapter, and as a student activity coordinator for IEEE APS-MTTS BD Joint Chapter. He is also an ambassador for IEEE Day 2024. His research interests include RFIC, bioelectromagnetics, microwave technology, antennas, phased arrays, and mmWave. He can be contacted at email: litonpaulete@gmail.com.